Research on Millimeter Wave Communication Interference Suppression of UAV Based on Beam Optimization

Weizhi Zhong(✉), Lei Xu, Xiaoyi Lu, and Lei Wang

College of Astronautics, Nanjing University of Aeronautics and Astronautics, Nanjing 210000, People's Republic of China
zhongwz@nuaa.edu.cn, 742426820@qq.com

Abstract. To support high data rate urgent, millimeter-wave (mmWave) UAV is considered and the beam forming technology which can further improve the mmWave communication performance is adopted. In the scene of mmWave communications for UAV group, the interference signal from other UAV and the reflected signal from the airframe can cause the communication quality to decrease. Therefore, it is very important to study the beam anti-interference performance based on the beam optimization. In this paper, a spatial interference channel model is established for UAV groups, and the expression of signal to interference plus noise ratio (SINR) depended on codebook design and direction of arrival (DOA) is obtained. Based on this, the performance of the beam interference suppression based on codebook optimization is simulated and the results show that the proposed optimization method can effectively suppress the interference and improve the system performance.

Keywords: UAV · Millimeter wave · Beamforming · Anti-interference

1 Introduction

Unmanned aerial vehicles (UAVs) have received increasing attention in the past decade [1, 2], thanks to potential applications in reconnaissance, firefighting, aerial photo, remote sensing, disaster rescue, and others. With the increasingly mature of UAV technology, UAV group combat model has become a new trend, and the concept of UAV group in the field of defense and civilian has caused more and more attention. However, real-time image transmission, spectrum sensing, heterogeneous data fusion and other technologies employed in UAVs require large bandwidth support. For this reason, large bandwidth is quite needed in the communication of UAVs.

Millimeter wave's can significantly improve system capacity as abundant frequency spectrum resource exists in the mmWave frequency band [3]. The wavelength of mmWave is very small, which makes the antenna array can be concentrated in a very

L. Xu—Foundation of Graduate Innovation Center in NUAA (kfjj20171501) supported by "the Fundamental Research Funds for the Central Universities".

X. Gu et al. (Eds.): MLICOM 2017, Part II, LNICST 227, pp. 472–481, 2018.
https://doi.org/10.1007/978-3-319-73447-7_51

compact space, and because of this, the application of large-scale antenna arrays on UAVs is possible. Therefore, UAV group communication based on the bandwidth of mmWave gradually attracted the attention of researchers [2]. However, when considering mmWave communication, an immediate concern is the extremely high propagation loss, since Friis' transmission law states that the free space omnidirectional path loss grows with the square of the carrier frequency. Fortunately, the small wavelength of mmWave signals also enables greater antenna gain for the same physical antenna size [4]. In addition, the Doppler effect as a result of UAV movement may not be catastrophic when high gain directional transmission is used [5]. For these reasons, mmWave UAV communications needs to be realized by large-scale array antenna.

For UAV group internal communication, the performance is affected by the more serious interference, mainly from signal send by other UAVs and the phenomenon of signal reflections and scattering [3, 6]. As a result, the degree of the interference is closely related to the relative position of UAV and the density of the UAV groups. In the past, there have been few studies on mmWave UAV communications, especially for beamforming interference suppression and real-time beam matching. Therefore, in this paper, for the UAV group communication environment, the interference characteristics are analyzed, the spatial interference channel model is established, and according to these, the SINR associated with the codebook and the direction of the DOA is obtained. Hence, the interference suppression based on codebook optimization is simulated and analyzed, which is the basis for the improving of beam optimization algorithm.

2 Interference Channel Model in UAV Group Environment

2.1 UAV Communication Scene

A typical UAV cellular network is shown in Fig. 1, where the base station (BS) is mounted on a flying UAV in the air, and mobile stations (MS) are distributed at low altitude or on the ground. The UAV group contains two kinds of communication links, one is responsible for UAV control and state information transmission, and the amount

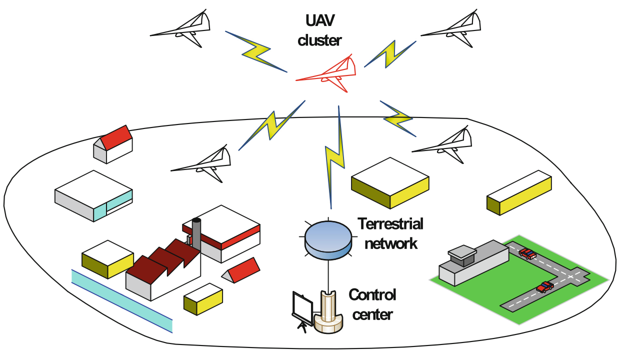

Fig. 1. UAV communication scenario

of data transmitted on this link is small. The other one is the information transmission link, which plays a major role in the mission implementation. On this link, large video monitoring traffic data from many camera sensors need to be collected and sent to other UAVs. Therefore, mmWave technology is mainly used in the second link. For information transmission link, when the commander establishes a contact with a UAV, the multipath reflection of the transmitted information and the information from other UAVs become the source of interference. Then, according to the specific position of the UAV, the interference model is modeled and the transmission channel coefficient is determined, and based on this the SINR is achieved.

2.2 The Interference Model of UAV Group

Let the signal of interest as $d(t)$, the arrival direction of it is θ_d, and the signal of unexpected can be expressed as $\mathrm{i}_j(t), j = 1, 2, \ldots, J$, these undesired signals are regarded as interference. The noise on each channel is the additive white Gaussian noise (AWGN), with mean equal to 0 and the variance of σ^2. Under the above conditions, the received signal of the specified UAV can be described as follow

$$
\begin{aligned}
y(t) &= \boldsymbol{w}^H \boldsymbol{x}(t) \\
&= \boldsymbol{w}^H \left[\boldsymbol{h}_d d(t) \boldsymbol{w}_d + \sum_{j=1}^{J} \boldsymbol{h}_j i_j(t) \boldsymbol{w}_j + \boldsymbol{n}(t) \right]
\end{aligned} \tag{1}
$$

Where $\boldsymbol{n}(t)$ is the AWGN with mean 0 and variance σ^2, $\boldsymbol{w}$ is the receiver beam weight vector, and $\boldsymbol{w}_x$ denotes beam weight vector of the transmitter. $\boldsymbol{h}_d$ is the channel state parameter of the desired signal, $\boldsymbol{h}_j$ is the channel state parameter of the interfering signal, both can be expressed as

$$
\begin{cases}
\boldsymbol{h}_d = \lambda_d \boldsymbol{a}(\theta_{Ad}) [\boldsymbol{a}(\theta_{Dd})]^H \\
\boldsymbol{h}_j = \lambda_j \boldsymbol{a}(\theta_{Aj}) \left[\boldsymbol{a}(\theta_{Dj})\right]^H
\end{cases} \tag{2}
$$

Where λ_x $(x \in \{d, j\})$ represents the channel amplitude, θ_{Ax} and θ_{Dx} are the angles of transmit (AOA) and the direction of arrival (DOA) of the desired signal and the interference, respectively.

$\boldsymbol{a}(\theta)$ denotes the array response, which can be expressed as

$$
\boldsymbol{a}(\theta) = [1, \quad e^{-j\frac{2\pi}{\lambda} d \sin\theta}, \cdots e^{-j\frac{2\pi}{\lambda} d (M-1) \sin\theta}] \tag{3}
$$

Where M is the number of elements. As shown in formula (1), the received signal contains not only the desired signal but also the interference and the noise from other UAVs. Therefore, the expression of the SINR is very important for the measurement of the interference, and can lay the foundation for the future design of the interference suppression scheme.

According to the received signal expression in formula (1), the average received power of the N samples of the received signal can be described as

$$
\begin{aligned}
P(\omega) &= \frac{1}{N}\sum_{t=1}^{N}|y(t)|^2 \\
&= \frac{1}{N}\left|\boldsymbol{w}^H\boldsymbol{h}_d\boldsymbol{w}_d\right|^2\sum_{t=1}^{N}|d(t)|^2 + \frac{1}{N}\sum_{j=1}^{J}\left|\boldsymbol{w}^H\boldsymbol{h}_j\boldsymbol{w}_j\right|^2\sum_{t=1}^{N}\left|i_j(t)\right|^2 + \left\|\boldsymbol{w}^H\right\|^2\frac{1}{N}\sum_{\boldsymbol{t=1}}^{\boldsymbol{N}}\boldsymbol{n}(t).
\end{aligned} \tag{4}
$$

Therefore, according to formula (4), the SINR can be expressed as

$$
SINR = \frac{\frac{1}{N}\left|\boldsymbol{w}^H\boldsymbol{h}_d\boldsymbol{w}_d\right|^2\sum_{t=1}^{N}|d(t)|^2}{\frac{1}{N}\sum_{j=1}^{J}\left|\boldsymbol{w}^H\boldsymbol{h}_j\boldsymbol{w}_j\right|^2\sum_{t=1}^{N}\left|i_j(t)\right|^2 + \left\|\boldsymbol{w}^H\right\|^2\frac{1}{N}\sum_{\boldsymbol{t-1}}^{\boldsymbol{N}}\boldsymbol{n}(t)}. \tag{5}
$$

As shown in Eq. (5), the value of SINR depends on the noise and interference. When the noise value is constant, the interference item determines the value of SINR. The number of disturbances is related to the weight of the beam design and the number of interference. Meanwhile, the numerical value of interference depends on the quantity and density of the UAVs, and weight $\boldsymbol{w}_m$ depends on the codebook design. Therefore, optimizing the codebook is critical to the interference suppression.

3 Uniform Linear Array Beam Optimization for mmWave

There are three kinds of millimeter-wave beam optimization methods. The first one is loading-window designing method, that is, changing the amplitude without adjust the direction, and achieving the side lobe suppression by amplitude-weighted. The second one is based on the optimization of the codebook design, that is, through the codebook design [8], to obtain better beam characteristics and array gain. The third one is window function based codebook design, that is, fusion window function and codebook design to improve the performance of the interference reduction.

3.1 Beam Optimization Based on Window Function

In this paper, the uniform linear array (ULA) is adopted. The structure of the antenna is shown in Fig. 2.

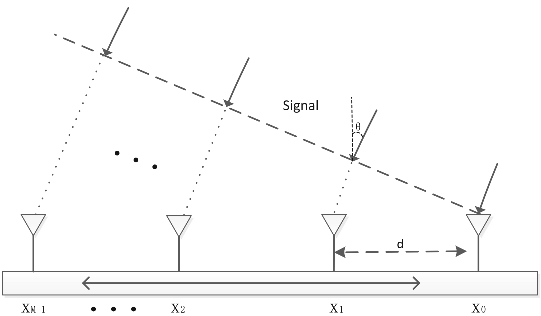

Fig. 2. Structure of the ULA

x_m stands for antenna array element, and θ represents the AOA [6], the time delay of the m-th element is expressed as follow

$$\tau_{\mathrm{m}}(\theta) = -(x_m \sin\theta)/c, m = 0 : M - 1. \quad (6)$$

The beam response can be described as

$$p(\theta) = w^H \alpha(\theta) = \sum_{m=0}^{M-1} w_m^* e^{-jw\tau_m(\theta)} = \sum_{m=0}^{M-1} w_m^* e^{j\frac{2\pi}{\lambda}md\,\sin\theta}. \quad (7)$$

Where w^H is the weight vector, which can be a window function, or a codebook design, and this is the focus of the paper. $\alpha(\theta)$ is the array response.

Window function optimization is to suppress the side lobes by the design of the weight vector w^H, which is only associated with amplitude changing. Common window functions have many different window types, such as binomial weighting function, Hamming weighting function, Hanning window function and Blackman window function. The optimization results of the window function is shown in Fig. 3. The comparison between the Chebyshev window and the uniform window is shown in Fig. 3(a), and the simulation results of the Hanning window and the uniform window is shown in Fig. 3(b). Through the window function optimization, the sidelobes can be effectively inhibited and the main lobe gain is improved. The simulation results also show that, the Chebyshev window and the Hanning window make the main lobe width changed.

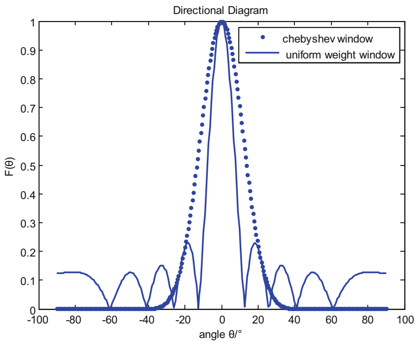

(a)

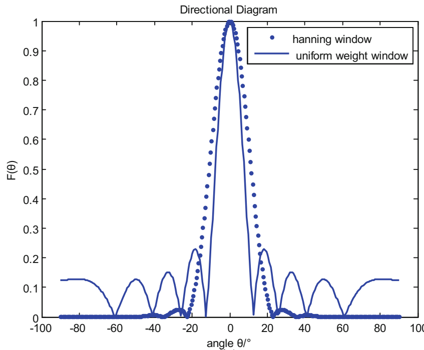

(b)

Fig. 3. Direction diagram with various windows

3.2 Beam Optimization Based on Codebook Design

The optimization of normalized weight vectors is an important part of codebook design. codebook $\mathbf{W} = [\mathbf{w}_1, \ldots, \mathbf{w}_K] \in \mathbf{C}^{M \times K}$ is consisted of K beamforming vectors $\mathbf{w}_m$, which produced by phase shifter, and $\mathbf{w}_m = [w_1, \ldots, w_M]^T \in \mathbf{C}^M$. Every element in the matrix is expressed as

$$w_m = e^{j\varphi_m}, \varphi_m \in \left\{0, 2\pi/2^B, \ldots, 2\pi(2^B - 1)/2^B\right\}. \tag{8}$$

In formula (8), B can be any integer, and the two codebook designs mentioned below are based on the change in B.

Taking the design of the beam codebook in the IEEE802.11.3c standard as an example, in which the beam vectors are given by column vectors of the following matrix

$$\begin{array}{l} w(m,k) = j^{fix\left(\frac{m \times \mathrm{mod}(k+(K/2),K)}{K/4}\right)} \\ m = 0 : M-1;\ k = 0 : K-1; \end{array} \tag{9}$$

Where M is the number of elements, and K denotes the number of beams. The function fix() returns the biggest integer which is smaller or equal to its value. M = mod(x,y) is defined as $x - n_1 y$, where n_1 is the nearest integer less or equal to x/y. The essence of the 3C codebook is that it composes of four complex numbers with a phase interval of 90°. To meet the low power consumption and complexity requirements, the codebook changes the phase shift without adjusting the amplitude, and its beam pattern is shown in Fig. 4(a).

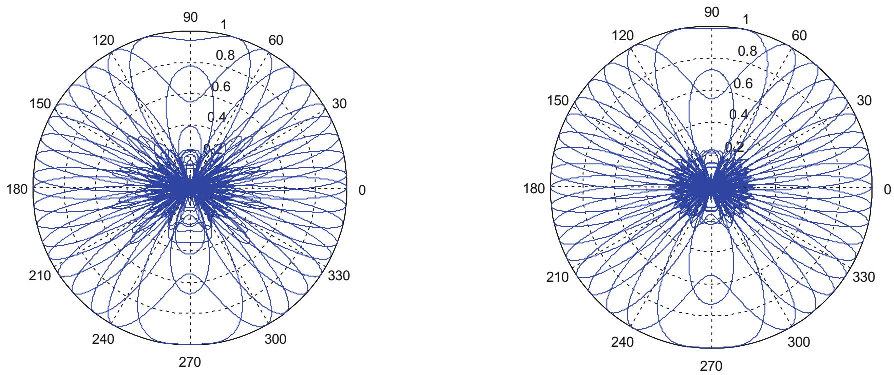

(a) 3C codebook (b) N phase codebook

Fig. 4. Normalized polar coordinate beam pattern

This paper also introduces an improved N-phase codebook design scheme [4], which is an extension of the 3C codebook. Compared with the 3C codebook, the phase interval between the N-phase codebook weights is further reduced, the beam is finer and the sidelobe gain can be further suppressed. The N-phase beam codebook can be expressed as follow

$$\begin{array}{l} w(m,k) = e^{j\frac{2\pi}{N} fix\left(\frac{m \times \mathrm{mod}(k+(K/2),K)}{K/N}\right)} \\ m = 0 : M-1; k = 0 : K-1 \end{array} \tag{10}$$

N represents the number of phases. Figure 4(b) shows the beam pattern generated by the N-phase codebook when N = 8.

The simulation results show that the beam phase adjustment can be done by codebook design, while the sidelobe interference of N phase codebook is significantly smaller than that of 3C codebook, and the performance can be improved remarkably. In [8], the design principle of complex codebook is introduced systematically, and the codebook scheme for surface antenna is also proposed. It is proved that the codebook design is one of the most important idea to solve the beamforming problem in future development [9].

3.3 Codebook Design Based on Window Function

Figure 5 is the beam pattern of 3C codebook and N phase codebook after the windowing. Figure 5(a) is the beam pattern of 3C codebook with Chebyshev window, and Fig. 5(b) is beam pattern of N phase codebook with Chebyshev window. Figure 5(c) is the beam pattern of 3C codebook with Hanning window, and Fig. 5(d) is the N phase codebook with Hanning window. Combined with Fig. 3 it is not difficult to find that, the codebook design with the window function can not only change the beam direction, but also further inhibit the sidelobes. Certainly, it needs further analysis to determine the specific performance changes.

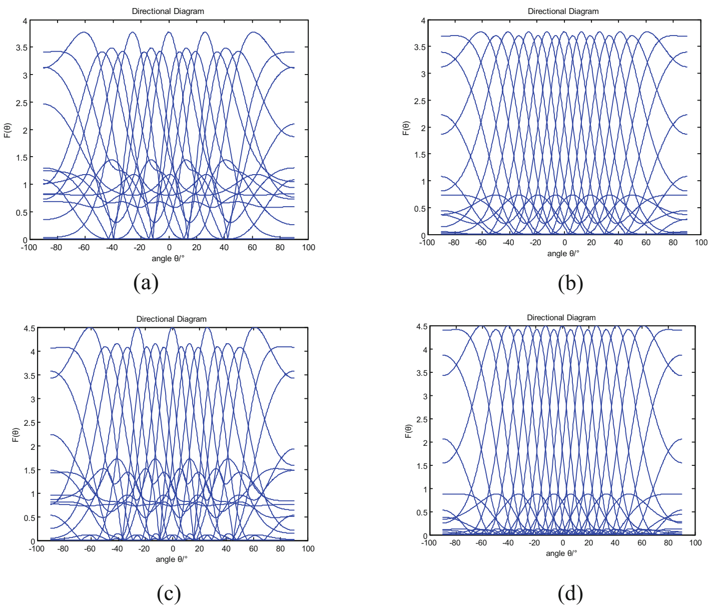

Fig. 5. Codebook beam pattern with windows

4 Interference Suppression of UAV Group Based on Beam Optimization

Based on the above expression of SINR and the beam optimal design schemes, in this section, the interference suppression method for UAV group communication based on beam optimization is simulated and discussed.

As shown in Eq. (5), the SINR is related to the weight vector $\boldsymbol{w}_m$, and when the noise is constant, the interference can be effectively suppressed by optimizing the weight of the codebook. As shown in Sect. 3, the codebook design based on window function has better interference suppression effect compared to the simple loading-window and codebook design. Therefore, based on the derived SINR expression, the interference suppression performance of various codebook optimization schemes can be simulated and analyzed.

The simulation conditions are as follows. Assuming that other UAVs are randomly determined by the Poisson distribution around the command machine, the communication channel does not consider the attenuation and other factors, and only the existence of AWGN is taken into account. The interference mainly comes from other UAV communication signal, and the interference signal power setting is the same. The signal-to-noise ratio (SNR) is set to a certain value, and the anti-interference performance of the system under different beam optimization schemes is studied by increasing the number of UAV interfering devices from 1 to 50. The simulation parameters are shown in Table 1.

Table 1. Communication parameters in UAV group

Signal frequency	60 GHz
Signal transmission rate	100M bit/s
Bandwidth of the signal	1.08G
Channel condition	Gaussian channel with SNR = 10 dB
Relative rate between UAVs	0 m/s
Location distribution of UAVs	Poisson distribution
Type of antenna	Transmitter-no directional antenna; Receiver-antenna array

It is known in expression (5) that the SINR decreases as the interference increases. The number of disturbances is closely related to the density of the UAVs group and the number of interference. The interference power depends on the transmission power and the distance between the UAVs. When the number of disturbances and interference power is constant, the SINR of the received signal can be influenced by the optimized design of the beam.

As shown in the Fig. 6(a), the interference suppression performance of the windowless N-phase codebook is better than that of the 3C codebook without window. As the N-phase codebook is designed with more phase values, then better beam pattern can be obtained and the shortage of the 3C codebook is overcame. N-phase codebook with any window has the better performance than both N-phase codebook without window

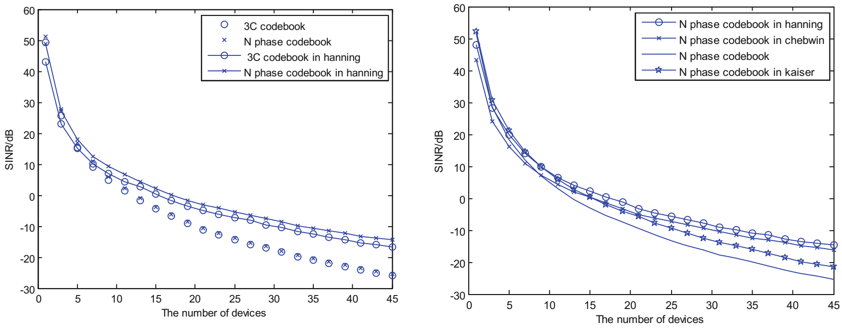

(a) (b)

Fig. 6. SINR for various beam designs

and 3C codebook with the same window. It happens as the improving of the side-lobe suppression enhances the anti-interference performance [4]. As shown in Fig. 6(b), among the all optimization schemes, N-phase codebook based on Hanning window has the best interference suppression ability.

5 Conclusion

UAVs group communication based on millimeter-wave is now widely concerned by researchers. However, the interference among the UAVs has significant influence on system performance. Therefore, focusing on the millimeter-wave UAVs communication, this paper establishes the spatial interference channel model of the UAVs group, obtains the SINR expression based on the codebook and the direction of the DOA, and then several typical optimization schemes is proposed. Simulation results show that, the proposed optimal scheme can further depress the interference and effectively improve the communication performance.

References

1. Yong, Z., Zhang, R., Teng, J.L.: Wireless communications with unmanned aerial vehicles: opportunities and challenges. IEEE Commun. Mag. **54**(5), 36–42 (2016)
2. Xiao, Z.Y., Xia, P., Xia, X.G.: Enabling UAV cellular with millimeter-wave communication: potentials and approaches. IEEE Commun. Mag. **54**(5), 66–73 (2016)
3. Roh, W., Seol, J.Y.: Millimeter-wave beamforming as an enabling technology for 5G cellular communications: theoretical feasibility and prototype results. IEEE Commun. Mag. **52**(2), 106–113 (2014)
4. Zou, W.X., Cui, Z., Li, B.: Beamforming codebook design and performance evaluation for 60 GHz wireless communication. In: IEEE International Symposium on Communications and Information Technologies, pp. 30–35. IEEE Press, Hangzhou (2011)

5. Vutha, V., Heath, R.-W.: Basic relationship between channel coherence time and beamwidth in vehicular channels. In: IEEE Vehicular Technology Conference, pp. 1–5. IEEE Press, Boston (2015)
6. Hansen, R.-C.: Phased Array Antennas, 2nd edn. Wiley, Hoboken (2009)
7. Jin, S., Zhang, X.L., Qi, Z.: A statistical model for the UAV communication channel. Acta Aeronautica Et Astronautica Sinica **25**(1), 62–65 (2004)
8. Song, J.H., Choi, J., Love, D.-J.: Common codebook millimeter wave beam design: designing beams for both sounding and communication with uniform planar arrays. IEEE Trans. Commun. **65**(4), 1859–1872 (2017)
9. Noh, S., Zoltowski, M.-D, Love, D.-J.: Multi-resolution codebook and adaptive beamforming sequence design for millimeter wave beam alignment. IEEE Trans. Wirel. Commun. 1 (2017)